Pelvic Fracture Reduction Planning Based on Morphable Models and Structural Constraints

Sutuke Yibulayimu[1], Yanzhen Liu[1], Yudi Sang[3], Gang Zhu[3], Yu Wang[1(✉)], Jixuan Liu[1], Chao Shi[1], Chunpeng Zhao[2], and Xinbao Wu[2]

[1] Key Laboratory of Biomechanics and Mechanobiology, Ministry of Education, Beijing Advanced Innovation Center for Biomedical Engineering, School of Biological Science and Medical Engineering, Beihang University, Beijing 100083, China
{sutuk,wangyu}@buaa.edu.cn
[2] Department of Orthopaedics and Traumatology, Beijing Jishuitan Hospital, Beijing, China
[3] Beijing Rossum Robot Technology Co., Ltd., Beijing, China

Abstract. As one of the most challenging orthopedic injuries, pelvic fractures typically involve iliac and sacral fractures as well as joint dislocations. Structural repair is the most crucial phase in pelvic fracture surgery. Due to the absence of data for the intact pelvis before fracture, reduction planning heavily relies on surgeon's experience. We present a two-stage method for automatic reduction planning to restore the healthy morphology for complex pelvic trauma. First, multiple bone fragments are registered to morphable templates using a novel SSM-based symmetrical complementary (SSC) registration. Then the optimal target reduction pose of dislocated bone is computed using a novel articular surface (AS) detection and matching method. A leave-one-out experiment was conducted on 240 simulated samples with six types of pelvic fractures on a pelvic atlas with 40 members. In addition, our method was tested in four typical clinical cases corresponding to different categories. The proposed method outperformed traditional SSM, mean shape reference, and contralateral mirroring methods in the simulation experiment, achieving a root-mean-square error of 3.4 ± 1.6 mm, with statistically significant improvement. In the clinical feasibility experiment, the results on various fracture types satisfied clinical requirements on distance measurements and were considered acceptable by senior experts. We have demonstrated the benefit of combining morphable models and structural constraints, which simultaneously utilizes cohort statistics and patient-specific features.

Keywords: Surgery planning · Pelvic fracture · Morphable models

Supplementary Information The online version contains supplementary material available at https://doi.org/10.1007/978-3-031-43996-4_31.

© The Author(s), under exclusive license to Springer Nature Switzerland AG 2023
H. Greenspan et al. (Eds.): MICCAI 2023, LNCS 14228, pp. 322–332, 2023.
https://doi.org/10.1007/978-3-031-43996-4_31

1 Introduction

Reduction planning is a crucial phase in pelvic fracture surgery, which aims to restore the anatomical structure and stability of the pelvic ring [21]. Traditional reduction planning relies on surgeons to form a "mental" plan through preoperative CT images, and the results are dependent on the surgeon's skill and experience. Computer-aided diagnosis (CAD) tools have been used for reduction planning, by virtually manipulating 3D bone models [2,23]. For complex fractures, 3D manual planning is not only time-consuming but also error-prone [19]. An automatic reduction planning method that offers improvements in both accuracy and efficiency is in demand.

The most intuitive method for reduction planning is by matching the fracture surface characteristics [16,20]. However, these methods rely on the precise identification and segmentation of fracture lines, which is typically challenging, especially in comminuted fractures where small fragments are "missing". Template-based approaches avoid the fracture line identification process. These methods include the average template statically modeled from pelvic shapes [3] and the template mirrored from the healthy contralateral side [6,22]. The former is not adaptive to individual morphology, usually resulting in poor robustness. Whereas the latter can only handle iliac fractures and is limited by the fact that the two ilia are usually not absolutely symmetric [7]. In addition, the contralateral mirroring (CM) method faces a severe challenge in bilateral injuries, where the mirrored part cannot provide accurate references.

Han et al. [11] used a statistical shape model (SSM) for pelvic fracture reduction, which adaptively matches the target morphology of pelvic bone. However, differences in the shape and integrity of the model bone and target fragments challenge the accurate adaptation of the SSM. Although the SSM method applies to all situations, without fully utilizing the whole pelvic structure, including the symmetricity, it often presents lower robustness. A recent study have pointed out that the CM method achieved better results than the adaptable iliac SSM [14].

While the SSM method addresses the reduction within single bones, it does not apply well to inter-bone matching for joint dislocations [8]. Statistical pose model (SPM) was proposed to jointly model the similarity transformations between bones, and to decouple the morphology of the entire pelvis into single bone shape and inter-bone poses [10]. The SPM models the statistics of bone positions but ignores the details in the joint connections which has rich information useful for aligning the joint surfaces. An under-fitted SPM may result in poor joint alignment and overall pelvic symmetry, which are very important considerations in reduction surgery in clinical practice.

In this study, we present a two-stage method for automatic pelvic reduction planning, addressing bone fractures and joint dislocations sequentially. A novel SSM-based symmetrical complementary (SSC) registration is designed to register multiple bone fragments to adaptive templates to restore the symmetric structure. Then, an articular surface (AS) detection and matching algorithm is designed to search the optimal target pose of dislocated bones with respect to joint alignment and symmetry constraints. The proposed method was evaluated

in simulated experiments on a public dataset, and further validated in typical clinical cases. We have made our clinical dataset publicly available at https://github.com/Sutuk/Clinical-data-on-pelvic-fractures.

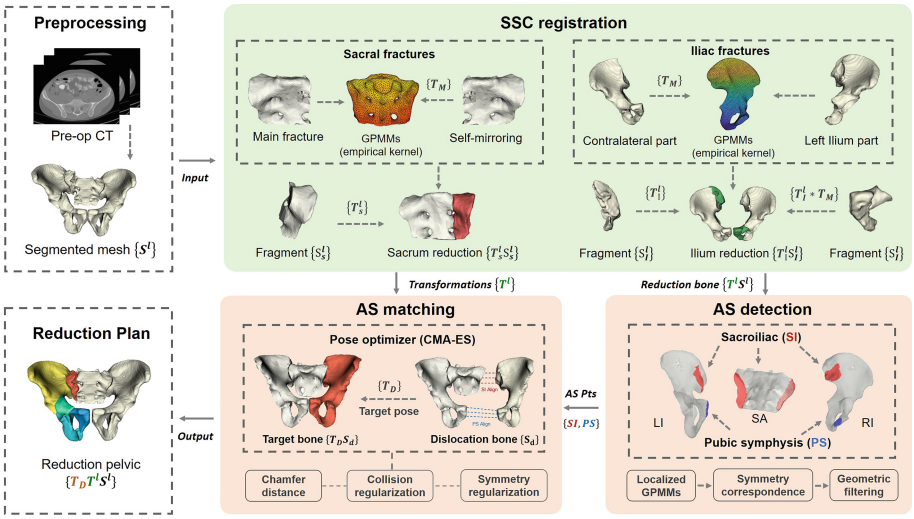

Fig. 1. Overview of the proposed reduction planning method for pelvic fracture surgery.

2 Method

As shown in Fig. 1, 3D models of the bone fragments in ilia and sacrum are obtained by semi-automatic segmentation [15]. Our automatic planning algorithm consists of two stages. The first stage computes the transformation of each bone fragment to restore single-bone morphology. The second stage estimates the target pose of each dislocated bone with respect to the whole pelvic anatomy.

2.1 Gaussian Process Morphable Models for Pelvic Bone

We use Gaussian process morphable models (GPMMs) [17] to model the shape statistics of pelvic bones. A healthy bone template is created for fractured fragments using **empirical kernel**, which enables the model to generate physiologically feasible bone morphology. In addition, **localized kernel** is used to create models with higher flexibility in order to approximate the morphology of the reduced/intact bone and then identify the pelvic AS areas.

Parameterized Model. The GPMMs of the left ilium and sacrum are modeled separately by first aligning bone segmentations to a selected reference Γ_R. A bone shape Γ_B can be obtained by warping the reference Γ_R with a deformation field $u(x)$. The GPMMs models deformation as a Gaussian process $GP(\mu, k)$ with a mean function μ and covariance function k, and is invariant to the choice of reference Γ_R. Parameterized with principal component analysis (PCA) in a finite dimension, the GPMMs can be written as:

$$\Gamma_B = \{x + \mu(x) + Pb \mid x \in \Gamma_R\}, \tag{1}$$

where P and b are the principal components and the weight vector, respectively. GPMMS modeled with the empirical kernel in a finite domain is equivalent to a statistical shape model (SSM), and the parameter is denoted as b_{SM}. The parameters of the localized model are denoted as b_{LC}.

Empirical Kernel for Fracture Reduction. A Gaussian process $GP(\mu_{SM}, k_{SM})$ that models the distinctive deformations is derived from the empirical mean $\mu(x) = \frac{1}{n}\sum_{i=1}^{n} u_i(x)$ and covariance function:

$$k_{SM}(x, y) = \frac{1}{n-1}\sum_{i=1}^{n} \left(u_i(x) - \mu_{SM}(x)\right)\left(u_i(y) - \mu_{SM}(y)\right)^T, \tag{2}$$

where n represents the number of training surfaces, and $u_i(x)$ denotes single point deformation on the i-th sample surfaces.

Localized Kernel for as Detection. In order to increase the flexibility of the statistical model, we limit the correlation distance between point clouds. The localized kernel is obtained by multiplying the empirical kernel and a Gaussian kernel $k_g(x, y) = \exp(-\|x - y\|^2/\sigma^2)$:

$$k_{LC}(x, y) = k_{SM}(x, y) \odot I_{3\times 3} k_g(x, y), \tag{3}$$

where $\odot$ denotes element-wise multiplication, the identity matrix $I_{3\times 3}$ is a 3D vector field, and σ determines the range of correlated deformations. The kernel is then used in AS detection.

2.2 Symmetrical Complementary Registration

A novel SSC registration is designed to register bone fragments to adaptive templates in joint optimization, which alternatingly estimates the desired reduction of fragments and solves the corresponding transformations. A bilateral supplementation strategy is used in model adaptation: mirrored counterparts are aligned to the target point cloud to provide additional guidance. In more detail, both the fragment and its mirrored counterpart are first rigidly aligned

to the GPMM with empirical kernel k_{SM}, using the iterative closest point (ICP) algorithm. Then, the GPMM is non-rigidly deformed towards the merged point clouds of the main fragment and its mirrored counterparts. During this step, the model's parameters b_{SM} are optimized using bi-directional vertex correspondences (target to source $v_{\rightarrow}(x)$ and backward $v_{\leftarrow}(x)$) based on the nearest neighbour. For each source point x, there is a forward displacement $\delta_{\rightarrow}(x) = v_{\rightarrow}(x) - x$, and one or more backward displacement $\delta_{\leftarrow}(x) = v_{\leftarrow}(x) - x$. The farthest point within the given threshold ε is selected as the corresponding point displacement $\delta(x)$ of the template:

$$\delta(x) = I\left(|\delta(x)| < \varepsilon\right) \max\left(|\delta_{\rightarrow}(x)|, |\delta_{\leftarrow}(x)|\right) + I\left(|\delta(x)| \geq \varepsilon\right) \mathbf{O}, \tag{4}$$

where I is the indicator function and $\mathbf{O}$ is a zeros vector. The optimal parameter $\hat{b}_{SM}$ of the statistical model can be calculated from Eq. (1), and is constrained within three standard deviations of the eigenvalue λ_i [1]:

$$\hat{b}_{SM} = \text{argmin}\{\delta(x) - \mu(x) - P b_{SM} \mid x \in \Gamma_R\}, \ |\hat{b}_{SM}| < \pm 3\sqrt{\lambda_i}. \tag{5}$$

The adaptive shape of the GPMM is regarded as the target morphology of a bone, and the fracture fragments are successively registered to the adaptive template to form the output of the first stage, reduction transformation T^l of each bone fragment S^l, $l = 1, ..., L$. As shown in Fig. 1, in the SSC registration stage, contralateral complementation and self-mirroring complementation are used for ilium and sacrum, respectively.

2.3 Articular Surface Detection and Matching

Articular Surface Detection. The AS of the sacroiliac (SI) joint and pubic symphysis (PS) are detected using the GPMMs for the ilia and sacrum, with the localized kernel. As indicated by the red and blue regions in Fig. 1 - AS detection, surface points in the joint regions are first manually annotated in the mean model template ($b_{LC} = 0$) and then propagated to each instance using non-rigid adaptation of GPMM model. The optimal parameter $\hat{b}_{LC}$ is obtained via the alternative optimization method in Sect. 2.2, and the marked points on the adaptive templates are mapped to the target bones as the AS regions. Due to the symmetric structure of the pelvis, we use a unilateral model to identify bilateral AS through mirror-flipped registration. Each AS landmark (vertex in mesh data) is associated with a normal vector. The average normal direction is computed from these vectors, and any surface landmark pairs deviating from this average direction are removed. The identified surface point sets are denoted as SI and PS.

Articular Surface Matching. For each joint, a ray-tracing collision detection algorithm is performed between opposing surfaces using surface normal [13]. Then, a cost function L_{local} is constructed to measure the degree of alignment

between two surfaces, including a distance term and a collision term. The former measures the Chamfer distance between complementary surfaces d_{cd} [4]. The latter uses an exponential function to map the IoU of the joint surface, so that slight collisions can be admitted to compensate for the potential inaccurate segmentation from the preprocessing stage.

$$\mathcal{L}_{local} = \ d_{cd}\left(S_1, S_2\right) + \gamma \cdot \exp\left(\frac{|S_1 \cap S_2|}{|S_1 \cup S_2|}\right), \tag{6}$$

where S_1 and S_2 are two sets of 3D points, and γ is a balancing weight for the collision term.

In addition to the local cost for each joint, a global cost measuring the degree of symmetry is used to regularize the overall anatomy of the pelvis:

$$\mathcal{L}_{global} = \frac{1}{|D_{\text{left}}|}||D_{\text{left}} - D_{\text{right}}||_2^2 + \langle \overrightarrow{V}_{PS}, \ \overrightarrow{V}_{SI} \rangle, \tag{7}$$

where the first term measures the paired difference between the point-wise distance within SI_{left} and SI_{right}. D_{left} and D_{Right} represent the distance between points in SI_{left} and SI_{right}, respectively. The second term measures the angle between the mean vector of the PS, denoted as $\overrightarrow{V}_{PS}$, and the mean vector of the bilateral SI joint $\overrightarrow{V}_{SI}$. The AS matching problem is formulated as optimizing the transformations with respect to the misalignment of PS and SI joints, plus the pelvic asymmetry:

$$\mathcal{L} = \mathcal{L}_{local}\left(SI_{left}\right) + \mathcal{L}_{local}\left(SI_{right}\right) + \mathcal{L}_{local}\left(PS\right) + \mathcal{L}_{global}, \tag{8}$$

where $\mathcal{L}_{local}\left(SI_{left}\right)$ or $\mathcal{L}_{local}\left(SI_{right}\right)$ can be a constant when the corresponding joint is intact, and can be omitted accordingly.

The cost function in Eq. (8) is optimized with respect to T_D, which determines the pose of the moving bone and its joint surfaces. The covariance matrix adaptation evolution strategy (CMA-ES) is used as the optimizer to avoid local minimum problem [12]. The final output point clouds of the pelvis is obtained by combining the transformation for the dislocated bone and the transformation for each fragment in the first stage $T_D T^l S^l$.

3 Experiments and Results

3.1 Experiments on Simulated Data

We evaluated the proposed fracture reduction planning method in a simulation experiment with leave-one-out cross-validation on the open-source pelvic atlas [9]. Extending from the simulation category in previous research [10], the current study simulated six types of fractures (the first column in Fig. 2), including single-bone fractures, joint dislocation, and combined pelvic trauma. The single-bone fractures include bilateral iliac wing fractures and sacral fractures,

and the combined simulation of pelvic trauma includes iliac fracture with dislocation (type A), sacral fracture with dislocation (type B), as well as iliac and sacral fractures with dislocation (type C). In total, 240 instances were simulated (6 fracture categories for each of the 40 samples). On the single-bone fracture data, the proposed SSC registration was tested against the mean shape reference and the SSM reference [11]. On the dislocation-only data, the proposed AS matching method was tested against the pelvic mean shape reference and contralateral mirroring (CM) [22]. On the combined-trauma data, the proposed two-stage method in Fig. 1 was tested against the pelvic mean shape reference and combined SSM and CM (S&C).

The Gaussian kernel parameter σ was set to 30, the collision regularization factor γ was set to 2, and the bidirectional correspondence threshold ε was set to 5. The accuracy of reduction was evaluated by the root-mean-square error (RMSE) on all fragments. Specifically, the average distance between the ground truth and the planned target location of all points was calculated.

As shown in Fig. 2, due to the strong individual variations, the mean reference was insufficient to cope with most fracture reduction problems, resulting in uneven fracture fragments and distorted bone posture. Without the symmetric complement, the SSM planning was more prone to large fragment gaps or overlaps than our method. Solely dependent on sacrum symmetry, the CM method often resulted in bone overlap or tilted reduction poses. The flaws of the cascaded comparison method were further magnified in combined pelvic fracture

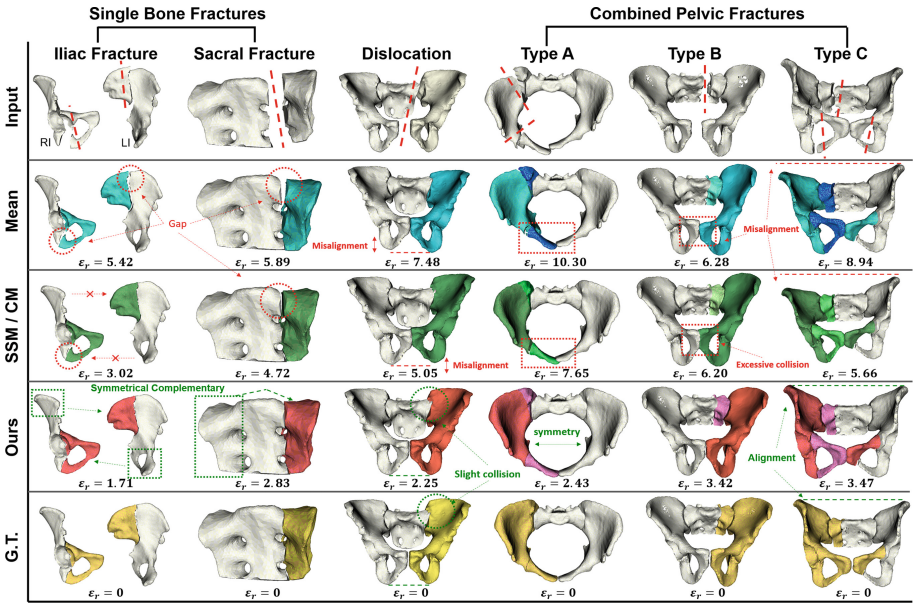

Fig. 2. Planning results on simulated data. Misalignments and good alignments are indicated by red and green dotted lines, respectively. (Color figure online)

reduction. Meanwhile, under the structural constraints, our method payed more attention to the overall symmetry, collision and articular surface anastomosis, and the results were closer to the ground truth.

As shown in Fig. 3, our method achieved the best median RMSE and interquartile range (IQR). Paired t-tests against other methods indicated statistical significance, with $p < 0.001$. For additional results, please refer to the Supplementary Material. The overall running time for the planning algorithm was 5 to 7 min on an Intel i9-12900KS CPU and an NVIDIA RTX 3070Ti GPU.

3.2 Experiments on Clinical Data

To further evaluate the proposed method on real clinical data, we collected CT data from four clinical cases (aged 34–40 years, one female), each representing a distinct type of pelvic fractures corresponding to the simulated categories. The data usage is approved by the Ethics Committee of the Beijing Jishuitan Hospital (202009-04). The proposed method was applied to estimate transformations of bone fragments to obtain a proper reduction in each case. Due to the lack of ground-truth target positions for fractured pelvis in clinical data, we employed

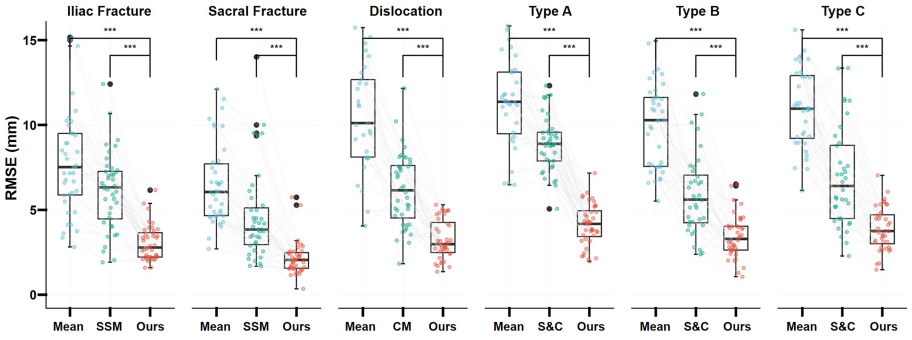

Fig. 3. Boxplots showing the RMSE between the planned target location and the ground truth on the simulated data. "$***$" indicates p-values less than 10^{-3} in t-tests.

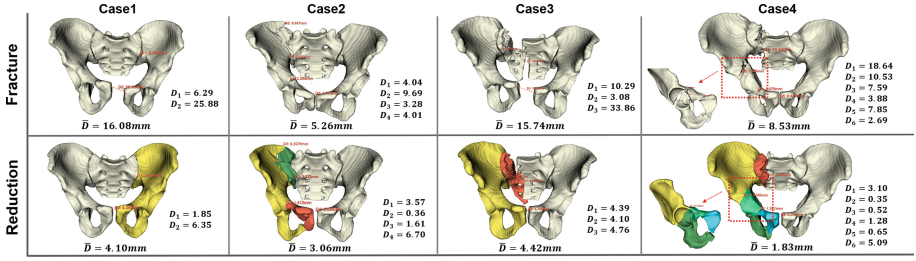

Fig. 4. Planning results on clinical data. D_i measures the distance between fragments in millimeter, and $\overline{D}$ is their average.

geometric measurements to evaluate the planning result. This evaluation method was inspired by Matta's trauma surgery criteria [18]. Surgeons manually measured the distances between all fragments and joints on a 3D slicer platform [5] by identifying a dislocated landmark pair across each fracture line or dislocated joint. The pelvic morphology in the planning result can be appreciated in Fig. 4. The measured distances between fragments or across joints are reduced to 1.8 to 4.4 mm. These planning results were examined by two senior experts and were deemed acceptable.

4 Discussion and Conclusion

We have proposed a two-stage method for pelvic fracture reduction planning based on morphable models and structural constraints. The SSM-based symmetrical complementary registration was successfully applied to both bilateral iliac and sacral fractures, which further extended the unilateral iliac CM reduction. Combining the SSM approach with symmetrical complementation provided more complete morphological guidance for model adaptation, and improved the registration performance significantly. The AS detection and matching method which combines local joint matching and global symmetry constraints achieved significantly higher accuracy than the pelvic mirroring reference. The proposed planning method also achieved satisfactory results on simulated data with combined pelvic trauma and real clinical cases.

We have demonstrated the synergy of the combined statistical model and anatomical constraints. In future work, we plan to further investigate this direction by incorporating feasibility constraints into SPM-based method to benefit from both cohort-based statistics and individual-specific matching criteria.

In the experiments, we simulated the most common fracture types and obtained the ground truth for evaluation. Due to the absence of ground truth in clinical data, we resort to an independent distance metric. We plan to test our method on more clinical data, and combine geometric measurements and manual planning for a comprehensive evaluation and comparison. We also intend to further automate the planning pipeline using a pelvic fracture segmentation network in future research to avoid the tedious manual annotation process.

Acknowledgements. This work is supported by the Beijing Science and Technology Project (Grants No. Z221100003522007 and Z201100005420033). We thank Runze Han et al. for their efforts on the open-source pelvic atlas.

References

1. Albrecht, T., Lüthi, M., Gerig, T., Vetter, T.: Posterior shape models. Med. Image Anal. **17**(8), 959–973 (2013). https://doi.org/10.1016/j.media.2013.05.010
2. Chowdhury, A.S., Bhandarkar, S.M., Robinson, R.W., Yu, J.C.: Virtual multi-fracture craniofacial reconstruction using computer vision and graph matching. Comput. Med. Imaging Graph. **33**(5), 333–342 (2009). https://doi.org/10.1016/j.compmedimag.2009.01.006

3. Ead, M.S., Palizi, M., Jaremko, J.L., Westover, L., Duke, K.K.: Development and application of the average pelvic shape in virtual pelvic fracture reconstruction. Int. J. Med. Robot. **17**(2), e2199 (2021). https://doi.org/10.1002/rcs.2199
4. Fan, H., Hao, S., Guibas, L.: A point set generation network for 3D object reconstruction from a single image. In: 2017 IEEE Conference on Computer Vision and Pattern Recognition (CVPR) (2017)
5. Fedorov, A., et al.: 3D slicer as an image computing platform for the quantitative imaging network. Magn. Reson. Imaging **30**(9), 1323–1341 (2012)
6. Fürnstahl, P., Székely, G., Gerber, C., Hodler, J., Snedeker, J.G., Harders, M.: Computer assisted reconstruction of complex proximal humerus fractures for preoperative planning. Med. Image Anal. **16**(3), 704–720 (2012). https://doi.org/10.1016/j.media.2010.07.012
7. Gnat, R., Saulicz, E., Biały, M., Kłaptocz, P.: Does pelvic asymmetry always mean pathology? Analysis of mechanical factors leading to the asymmetry. J. Hum. Kinet. **21**(2009), 23–32 (2009). https://doi.org/10.2478/v10078-09-0003-8
8. Han, R., et al.: Multi-body 3D-2D registration for image-guided reduction of pelvic dislocation in orthopaedic trauma surgery. Phys. Med. Biol. **65**(13), 135009 (2020). https://doi.org/10.1088/1361-6560/ab843c
9. Han, R., Uneri, A., Silva, T.D., Ketcha, M., Siewerdsen, J.H.: Atlas-based automatic planning and 3D-2D fluoroscopic guidance in pelvic trauma surgery. Phys. Med. Biol. **64**(9) (2019)
10. Han, R., et al.: Fracture reduction planning and guidance in orthopaedic trauma surgery via multi-body image registration. Med. Image Anal. **68**, 101917 (2021). https://doi.org/10.1016/j.media.2020.101917
11. Han, R., et al.: Multi-body registration for fracture reduction in orthopaedic trauma surgery. In: SPIE Medical Imaging, vol. 11315. SPIE (2020). https://doi.org/10.1117/12.2549708
12. Hansen, N., Müller, S.D., Koumoutsakos, P.: Reducing the time complexity of the derandomized evolution strategy with covariance matrix adaptation (CMA-ES). Evol. Comput. **11**(1), 1–18 (2003). https://doi.org/10.1162/106365603321828970
13. Hermann, E., Faure, F., Raffin, B.: Ray-traced collision detection for deformable bodies. In: International Conference on Computer Graphics Theory and Applications (2008)
14. Krishna, P., Robinson, D.L., Bucknill, A., Lee, P.V.S.: Generation of hemipelvis surface geometry based on statistical shape modelling and contralateral mirroring. Biomech. Model. Mechanobiol. **21**(4), 1317–1324 (2022). https://doi.org/10.1007/s10237-022-01594-1
15. Liu, P., et al.: Deep learning to segment pelvic bones: large-scale CT datasets and baseline models. Int. J. Comput. Assist. Radiol. Surg. **16**(5), 749–756 (2021). https://doi.org/10.1007/s11548-021-02363-8
16. Luque-Luque, A., Pérez-Cano, F.D., Jiménez-Delgado, J.J.: Complex fracture reduction by exact identification of the fracture zone. Med. Image Anal. **72**, 102120 (2021). https://doi.org/10.1016/j.media.2021.102120
17. Luthi, M., Gerig, T., Jud, C., Vetter, T.: Gaussian process morphable models. IEEE Trans. Pattern Anal. Mach. Intell. **40**(8), 1860–1873 (2018). https://doi.org/10.1109/tpami.2017.2739743
18. Matta, J.M., Tornetta, P.I.: Internal fixation of unstable pelvic ring injuries. Clin. Orthop. Relat. Res. (1976–2007) **329** (1996)
19. Suero, E.M., Hüfner, T., Stübig, T., Krettek, C., Citak, M.: Use of a virtual 3D software for planning of tibial plateau fracture reconstruction. Injury **41**(6), 589–591 (2010). https://doi.org/10.1016/j.injury.2009.10.053

20. Willis, A.R., Anderson, D.D., Thomas, T.P., Brown, T.D., Marsh, J.L.: 3D reconstruction of highly fragmented bone fractures. In: SPIE Medical Imaging (2007)
21. Yu, Y.H., Liu, C.H., Hsu, Y.H., Chou, Y.C., Chen, I.J., Wu, C.C.: Matta's criteria may be useful for evaluating and predicting the reduction quality of simultaneous acetabular and ipsilateral pelvic ring fractures. BMC Musculoskelet. Disord. **22**(1), 544 (2021). https://doi.org/10.1186/s12891-021-04441-z
22. Zhao, C., et al.: Automatic reduction planning of pelvic fracture based on symmetry. Comput. Methods Biomech. Biomed. Eng. Imaging Vis. **10**(6), 577–584 (2022). https://doi.org/10.1080/21681163.2021.2012830
23. Zhou, B., Willis, A., Sui, Y., Anderson, D.D., Brown, T.D., Thomas, T.P.: Virtual 3D bone fracture reconstruction via inter-fragmentary surface alignment. In: 2009 IEEE 12th International Conference on Computer Vision Workshops, ICCV Workshops, pp. 1809–1816 (2009). https://doi.org/10.1109/ICCVW.2009.5457502